Full Paper Transactions, SMiRT 28
Toronto, Canada, August 10-15, 2025

Numerical investigation of the behaviour of RC Wall under impact loads – application to the IMPACT III and IV experimental campaigns

Try MENG[1], David BOUHJITI[1], Nicolas PFEIFFER[2], Alix DE LA MESLIERE[2]

[1]The French Authority for Nuclear Safety and Radiation Protection, ASNR/DES/SES/LMAPS, Fontenay aux Roses (try.meng@asnr.fr)
[2]The French Authority for Nuclear Safety and Radiation Protection, ASNR/DES/SES/BEGC, Fontenay aux Roses

ABSTRACT

ASNR contributes to the IMPACT project organized by the Technical Research Center VTT (Finland) and funded by several institutions including ASNR. As part of the IMPACT project, reduced scale impact tests of reinforced concrete (RC) structures are carried out with combined bending and punching tests for different combinations of longitudinal and transverse reinforcement on the structural behaviour. This paper proposes a numerical approach to study the dynamic behaviour of RC walls based on the mock-up used within the IMPACT III and IV. The simulations proposed here consider a 3D numerical modelling for all specimens, which include the necessary supporting structure, RC wall and the projectile. The nonlinear behaviour of concrete and projectile are considered. Calculations are done through the explicit dynamic solver of LS-DYNA. Results analyses cover the damage distribution, the force history and displacement evolution during and after impact. Those results demonstrate that blind numerical modelling can be successfully achieved if the proper hypotheses are considered, especially regarding the boundary conditions. Nevertheless, it is observed that if the global behaviour can be assessed with good precision, the local behaviour of concrete is hard to predict and quantify for many reasons (continuous description of damage, post-processing of cracking from the damage and stress fields, local load redistribution and loss of stiffness, loss of sensors or absence of reliable measurements, etc.).

INTRODUCTION

The risk of impact effect has drawn attention in the verification of stability for the nuclear facilities. A series tests of IMPACT projects (II; III; IV) (Hakola, et al., 2010; Calonius, 2019; Fedoroff & Soares, 2024) is realized in order to understand the mechanical behaviour of the RC structure under the impact load varied through different configurations of the projectiles by thickness and velocity. IMPACT II is realized by projecting the missile to a thick steel plate; and means to record the impact force and to better characterized the numerical modelling of the projectile. In IMPACT III, the missile is projected to the RC walls. The objective is to study the response of the RC wall under the bending effect and combination of bending/shear effect. In IMPACT IV, the experiment is conducted by projecting the missile to two configurations of RC wall, which are at reference scale (GSX1R-S: 2m x 2m) and large scale (GSX1R-L: 3.5m x 3.5m). The objective is to observe the influence of scale effect to the response of dynamic behaviour of the structures.

In this paper, an investigation through the numerical modelling is developed in LS-DYNA (Live more Software Technology, 2020) with the representative studies cases of IMPACT III and IV. The simulation is made in 3D modelling, and the necessary elements such as: supporting structure, RC walls and projectile are modelled by the shell elements, solid elements and beam elements. The nonlinear constitutive law is considered for the concrete and the projectile elements. However, there exists different nonlinear constitutive law used for modelling the concrete material (Wu, et al., 2012; Trentacoste, 2007; Schwer, 2010) in LS-DYNA, and the most consistent constitutive law, MAT_159_CSCM (Novozhilov, et al., 2022; Trentacoste, 2007), found in the literature is used for modelling the concrete element in this work.

Furthermore, the contact modelling is also specially considered between RC wall and the projectile. The results of the simulation focus on the global and local behaviour of the structure. For the global behaviour, we considered the damage mapping of the RC wall, the deformed length of the projectile and the total measured force as the indicators to compare with those of the experiment. Regarding to the local behaviour, the displacement evolution; the strain evolution of the concrete and rebar are recorded from the sensors at different points.

OVERVIEW OF EXPERIMENTAL CAMPAIGN

Impact III & IV

In IMPACT III, the experimental platform is composed of the RC wall (2m x 2m) and the supporting structure in steel frame, see in Figure 1. The RC wall is installed between the steel frames and are tightened by the screws. Besides that, the horizontal steel pipes are connected from the steel frame to the back rock structure for absorbing the impact force into the rock during the test. Furthermore, the steel frame is placed on the block wood at each side. The missile is projected through a steel tube by an accumulator of compressed air for arriving an attempted velocity, see in Figure 2. Moreover, the missiles are projected in perpendicular to the RC wall.

Figure 1: the installation of RC wall in supporting structure, IMPACT III *(Calonius, 2019)*

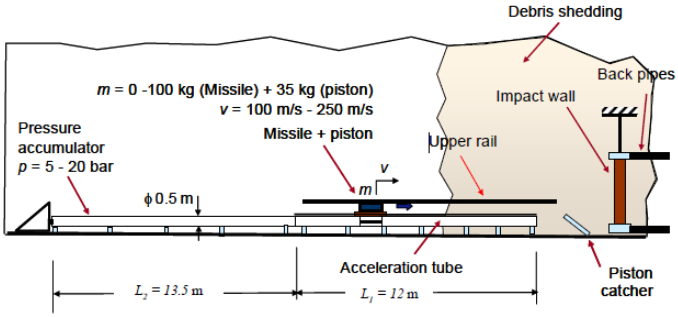

Figure 2: the installation for accelerator of the missile

Two experimental tests are performed under the platform of IMPACT IV, and the installation of the specimen is like those presented in IMPACT III, see in Figure 3. The geometry scale factor (1:1.75) is applied for two specimens: GSX1R-S for reference scale and GSX1R-L for large scale. It is worth to mention that the scale factor covers for the dimensions of the wall, reinforcement ratios and the thickness of the missile. Therefore, those experiments mean to investigate the influence of scale factor to the measured results.

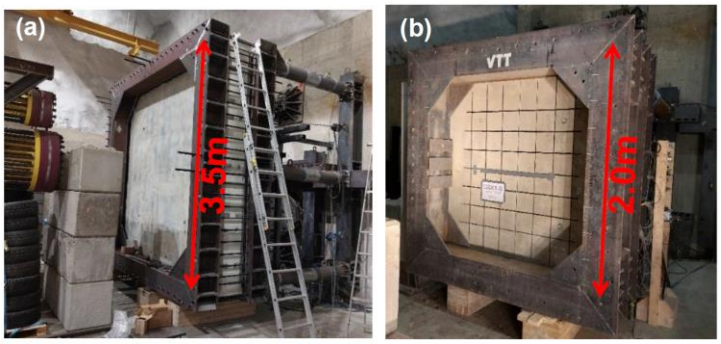

Figure 3: the installation of the experiment in IMPACT IV, (a): GSX1R-L, (b): GSX1R-S

The available measurements in both IMPACT III and IV include the total reaction forces (record on the steel pipes), displacements (sensors on the rear face), velocity of the missile, reinforcement strain and the visualization of the cracking patterns on the front and rear faces, see in Figure 4. Furthermore, the summary of the reinforcement percentage and geometrical dimensions are illustrated in Table 1.

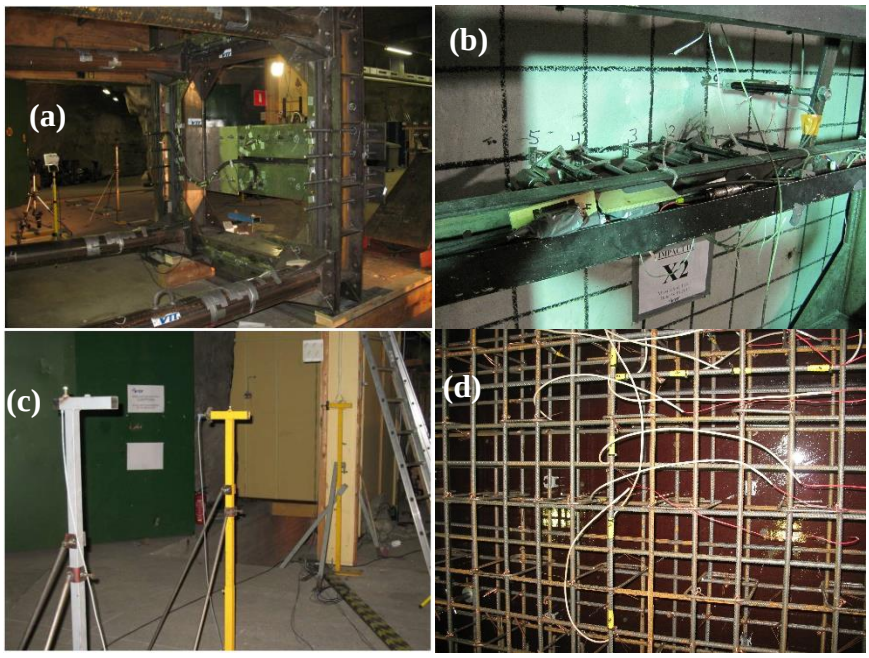

Figure 4: the sensors for measuring, (a) reaction force, (b) displacement, (c) velocity, (d) strain gauge

Table 1: the summary of reinforcement and geometry of the missile and concrete

	Test	Reinforcement		Missile					Concrete
		Bending	Shear (cm^2/m^2)	Thickness (mm)	Diameter (mm)	Length (mm)	Velocity (m/s)	Mass (kg)	Width x Heigh x Thickness
Impact III	X2	0.397%	17	3	256	1811	164.5	50	2m x 2m x 0.25m
	X6	0.397%	17	6.35	219.1	1304	166.7	50	2m x 2m x 0.25m
Impact IV	GSX1R-S	0.349%	17.45	4.57	219.1	1320	143	50	2m x 2m x 0.25m
	GSX1R-L	0.348%	21.15	8	390	1800	143	268	3.5m x 3.5m x 0.437m

OVERVIEW OF NUMERICAL MODEL

Geometry and mesh

As illustrated in Figure 5, the numerical mock-up for the IMPACT III and IV consists of the supporting structures, the RC wall and the missile. The supporting structures are modelled by shell elements for the steel frame and beam elements for the pipes. The RC wall is modelled by solid elements for the concrete and beam elements for the rebar. The missile is modelled by shell elements, and five points integrations are considered in the thickness. Globally, the mesh size is about 5cm for the concrete and 2cm for the rebar. Thus, the rebar is embedded into concrete through the constrained model (perfect bond). The mesh size of the missile is increased progressively from 1cm to 3cm between the head and bottom of the missile.

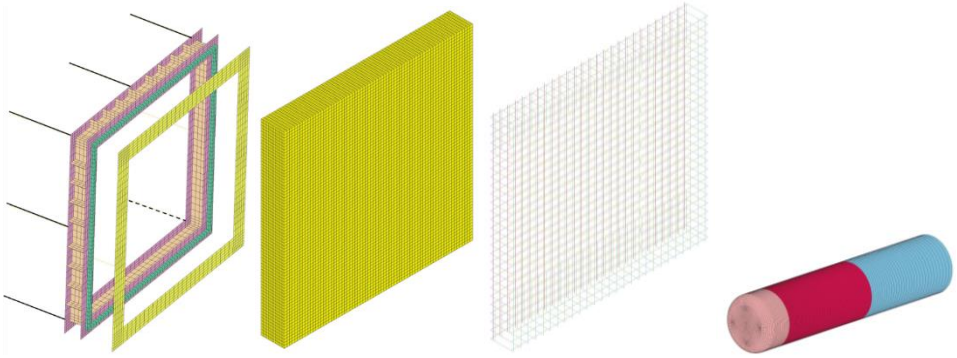

Figure 5: numerical mock-up of IMPACT IV (GSX1R-L)

Boundaries conditions

The boundaries conditions are applied to the supporting structure based on the configuration of the experiment, see in Figure 6. The extremities of the pipes are blocked in all displacements and rotations. On the bottom of the steel frame, the elements as seen in blue line are blocked in vertical displacement. To assure a symmetrical displacement in X direction, the elements at the red line (middle of steel frame) are blocked for the displacement in this direction. Besides that, a kinematic relationship is applied between the front steel frame (1) and the back steel frame (2) to displace all the same in Y direction. This simplification is made to consider the tightened screws that are not modelled explicitly.

Constitutive law

The constitutive laws used in different elements are illustrated in Table 2 as an example for IMPACT IV. The supporting structure is considered as an elastic behaviour, and the concrete is modelled by the damage constitutive law, called as MAT_CSCM_159. It is worth to mention that the literature (Wu, et al., 2012; OECD, 2012; Trentacoste, 2007) are found for the sensitivity analyses of the constitutive law for the concrete. Based on our feedback and the one of IMPACT partners, we adopt the CSCM_159 with an automatic generated parameters to our blind simulation. The rebar is modelled by a classic bi-linear plasticity law (MAT_003_Plastic_kinematic), and the missile is modelled by an elasto-plasticity law (MAT_024_linear_plasticity) where the hardening is considered directly through stress-strain curve measured from the sample scale.

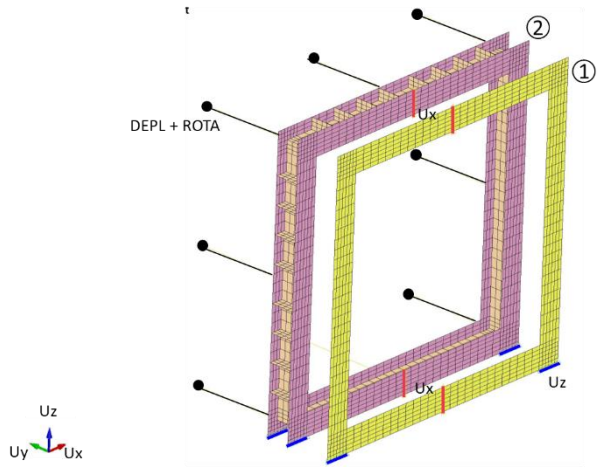

Figure 6: boundaries conditions of the supporting structures

Table 2: material constitutive law (IMPACT IV)

	LS-DYNA/material	
Concrete	CSCM_159: damage law	fc=63.3MPa; ft=4.29MPa; Ecm=33.9GPa
Rebar	003_Plastic kinematic: Bi-linear	E=200GPa; fy=514MPa (ϕ10); 573MPa (ϕ6); 538MPa (ϕ16)
Missile	024_linear plasticity	Carbon steel S355: fy=370MPa; E=200GPa
Steel frame	Elasticity	E=200GPa

Contact modelling

The contact of different elements is modelled with the nature of the installation of the experiment, see in Figure 7. Three contact models are adopted, which are tied surface contact for the steel plate embedded at all the border of the wall; automatic surface to surface contact is made between the steel frame and the steel plate; automatic single surface contact serves between the wall and the missile.

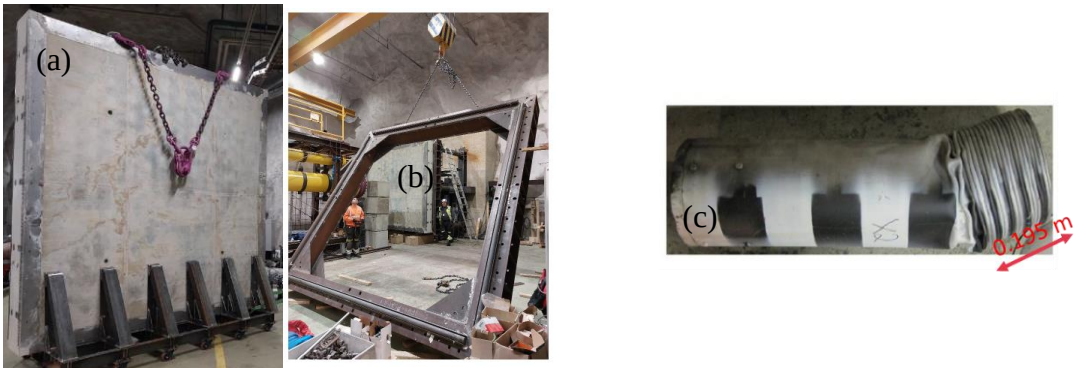

Figure 7: contact elements in the experimental test, (a) steel plate, (b) steel frame, (c) missile

RESULTS AND DISCUSSION

Deformed configuration

In Table 3, the deformed missiles are illustrated from the results of the simulation and experiment. It is observed that the missile is deformed into many folds, and the deformed lengths are compared between the simulation and experiment. In IMPACT III, the simulations of the tests X2 and X6 present the error at 11.2% and 23%, respectively. In IMPACT IV, the error between the simulation and experiment is about 13%. Those results are satisfying as far as our blind simulations are concerned; they can still be improved if one achieves a calibration of the parameters and accounts for the strain rate effect. Besides that, the scale factors (λ_{exp} , $\lambda_{simulation}$) are computed based on the deformed length from the tests GSX1R-S and GSX1R-L. Those factors are compared to the scale factor applied in the geometry (λ_p), and they present a coherent result where the deformed length seems to increase in proportional to scale factor in geometry. So, we can generally conclude to the scale factor objectivity given a 6% relative error.

Table 3: deformed missile, IMPACT III (X2, X6), IMPACT IV (GSX1R-S, GSX1R-L)

<table>
<tr><td>X2</td><td>X6</td></tr>
<tr><td> 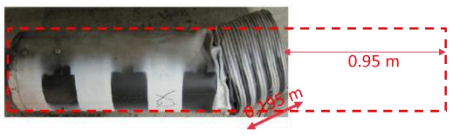

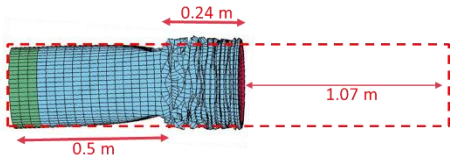
</td><td> 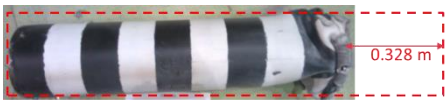

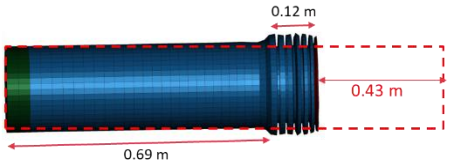
</td></tr>
<tr><td>error: 11.2%</td><td>error: 23%</td></tr>
<tr><td colspan="2"></td></tr>
<tr><td>GSX1R-S</td><td>GSXR-L</td></tr>
<tr><td> 

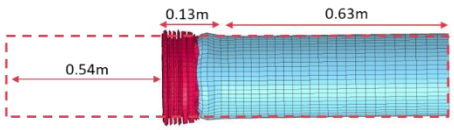
</td><td> 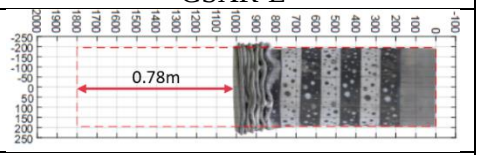

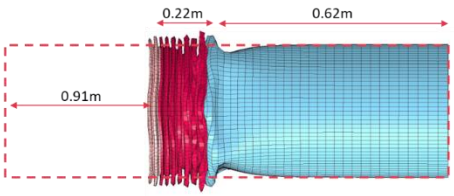
</td></tr>
<tr><td>error: 13%</td><td>error: 13.3%</td></tr>
<tr><td colspan="2">λ_{exp}=0.78/0.47=1.65 Vs λ_p=1.75
$\lambda_{simulation}$=0.91/0.54=1.68 Vs λ_p=1.75</td></tr>
</table>

Damage mapping

The damage distribution and cracking pattern are presented in Table 4 for the tests in IMPACT III. The simulation estimates the damage zones that are like the cracking map of the experiment. At the front face, the damage is focused on the middle of the wall (targeted point). At the rear face, the damage forms as a

cross line through the middle of the wall. Furthermore, the damage mapping is more important in X6, and this is because the thickness of the missile (see Table 1) is more significant, thus, it is more rigid.

In Table 5, the damage distribution and cracking pattern are illustrated for the tests of IMPACT IV. The damage zones on the front and rear face detected by the simulation are always coherent to those observed from the experiment. From the experiment, we could observe the erosion of some concrete elements on the rear face. But this effect has not been included in the current simulation (no erosion in our model).

Table 4: Damage distribution (simulation) and cracking pattern (experiment) for IMPACT III

Simulation	Experimentation
Test X2	
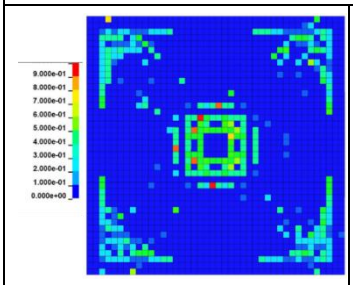	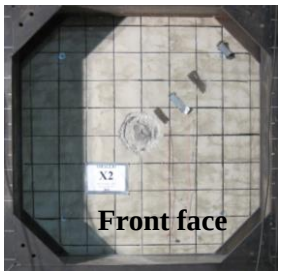
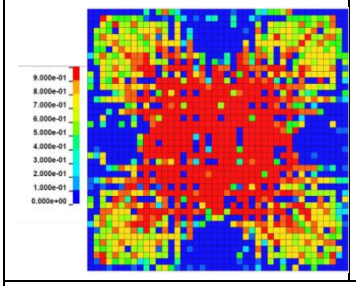	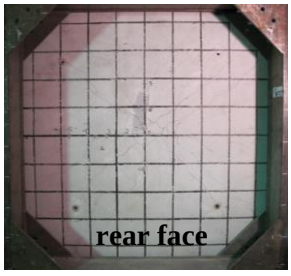
Test X6	
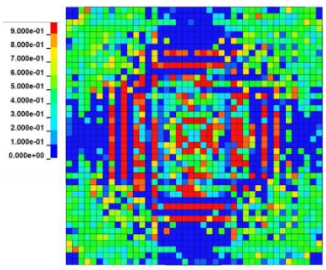	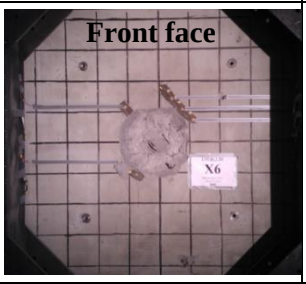
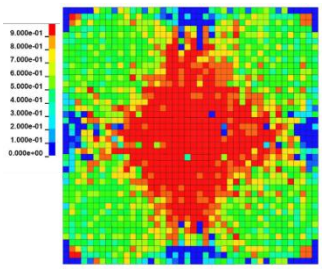	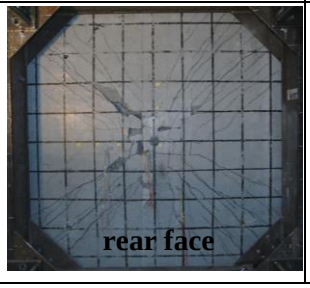

Table 5: Damage distribution (simulation) and cracking pattern (experiment) for IMPACT IV

Simulation	Experimentation
GSX1R-S	
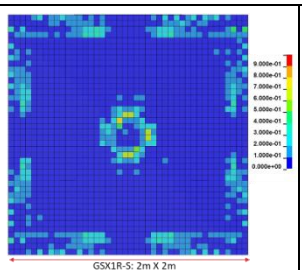	
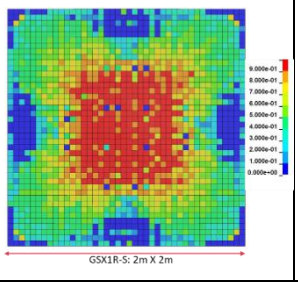	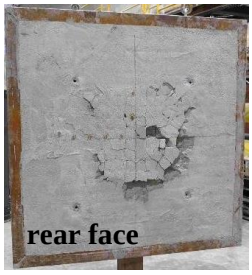
GSX1R-L	
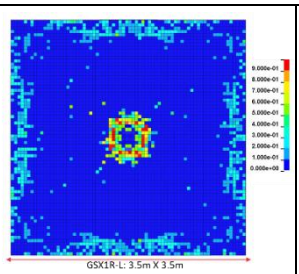	
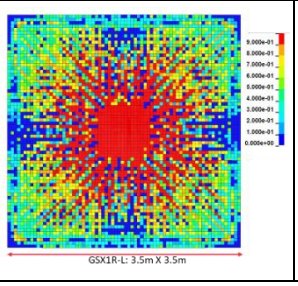	

Total force

In Table 6, the total force is measured from the back pipes, and the contact force is not available since there is no force transducer installed on the concrete. The reaction forces estimated by the simulation provide a similar tendency by comparing to the experiment. In IMPACT III, the maximum forces present a good agreement between the simulation and the experiment. In IMPACT IV, the simulation seems to underestimate it for the reference scale (GSX1R-S), whereas the large scale (GSX1R-L) estimates a similar maximum force between the experiment and the simulation. Force is a derived quantity, therefore, it is scaled by powers of the scaling factor. The computation of the scaling factor (λ_{exp} , $\lambda_{simulation}$) based on the maximum force is compared to the scale factor applied to the geometry (λ_p) of the tests in IMPACT IV. It is observed that the simulation seems to respect the scaling factor law, whereas the experiment presents a gap about 30% between λ_{exp} and λ_p. So, the geometrical scale factor seems to apply to the total force given a certain relative error ranging from 5% to 30%. For the latter, it seems that experimental results are less coherent with the outcome of our numerical analysis. So, this point requires more in-depth analysis to explain the reasons behind such an important gap (state of sensors/forces from one impact test to the other, evolution of the boundary conditions, etc.).

Table 6: comparison force history between simulation and experiment

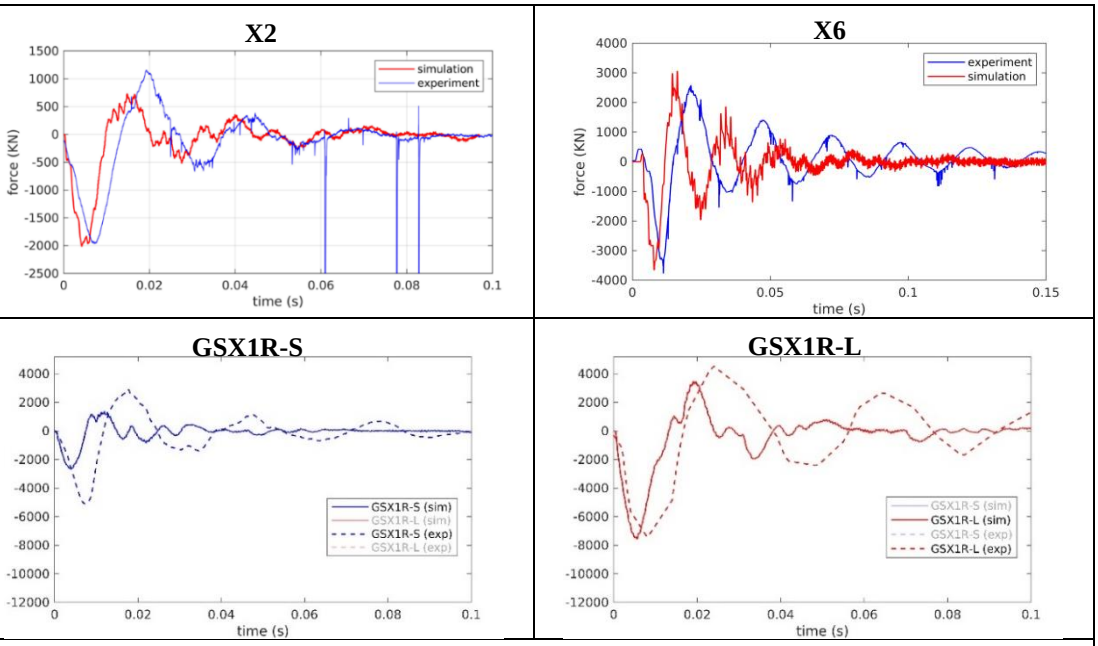

λ^2_{exp}=7780/5090 = 1.53 ➔ λ_{exp}=**1.23** Vs λ_p=**1.75**

$\lambda^2_{simulation}$=7504/2607 = 2.87 ➔ $\lambda_{simulation}$=**1.67** Vs λ_p=**1.75**

Displacement

The comparison of the displacements between the simulation and the experiment is illustrated in Table 7. As mentioned, the displacements are recorded at several points on the rear face of the wall. However, not all the points are correctly measured. In IMPACT III, the displacements at the central point are plotted, and the simulations underestimate it by 20% for X2 and about 4 times for X6. In IMPACT IV, the displacements are compared for the available results at point D3. The simulations systematically underestimate by 2 to 3

times the measured maximum displacement. However, there exists uncertainties in the measured displacement due to the vibration effect on the supporting element of the displacement sensors.

Table 7: comparison displacement history between simulation and experiment

IMPACT III	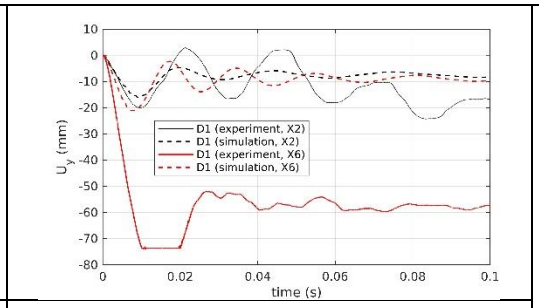	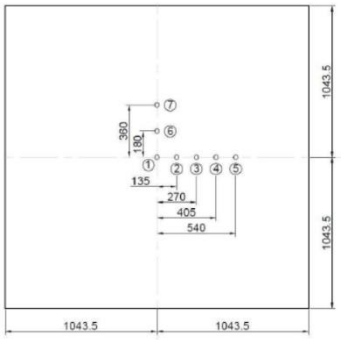
IMPACT IV	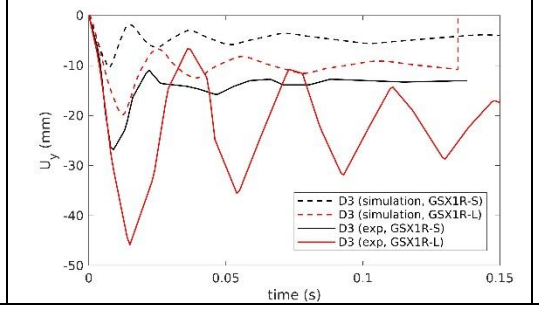	

CONCLUSION

The current paper proposes a modelling strategy for the blind simulation of RC concrete elements under impact loads. This is applied to the tests of IMPACT III and IV.

For the global behavior, simulations provide comparable results to the obtained experiments, including the deformed configuration of the missiles, damage distributions on the RC wall and the reaction force. The blind simulation predicts the deformed length of the missile with about 20% and 13% error, respectively in IMPACT III and IV. The damage distribution obtained by the simulation is coherent to the crack mapping. In IMPACT IV, the scaling factor law seems to be applicable on the global behavior including the deformed length of the missile and the reaction force, where the computed factors are like the geometrical scaling factor.

For the local behavior, the displacements of the wall are compared at different points, and the simulations mostly underestimate them by 2 to 3 times the displacements in the tests of IMPACT IV; gaps are even more important in test X6 of IMPACT III. Those differences might come from many sources including the uncertainty in the measured sensors and the limitation of the current simulation (less representative boundary conditions that are hard to control experimentally). According to our numerical results, the scaling law does not seem to be applicable to the local behavior of the structure, especially at the impact zone where the strong nonlinearity is obtained.

Eventually, such numerical simulations are possible for further improvement through the calibration on certain parameters in the constitutive law, strain rate effect on the material properties, bond-slip model at the rebar-concrete interface and the consideration of the erosion elements in the concrete. Besides that,

sensitivity analysis on the input parameters and the mesh size shall be considered for the continuation of this research work.

REFERENCES

Calonius, K., 2019. *IMPACT III - combined bending and punching tests,* Espoo: VTT.
Fedoroff, A. & Soares, G., 2024. *IMPACT IV - NEREID GSX1 test set,* Helsinki: VTT.
Hakola, I., Saarenheimo, A., Vepsä, A. & Halonen, M., 2010. *Impact Force Plate Tests Results in 2009 and 2010, Part 3,* Espoo: VTT.
Live more Software Technology, (., 2020. *LS-DYNA Keyword user's manual,* s.l.: ANSYS Company.
Novozhilov, Y. V., Dmitriev, A. N. & Mikhaluk, D. S., 2022. Precise Calibration of the Continuous Surface Cap Model for Concrete Simulation. *Buildings,* 12(5).
OECD, 2012. *Improving Robustness Assessment Methodologies for Structures Impacted by Missile (IRIS_2010),* s.l.: Nuclear Energy Agency / Committee on the Safety of Nuclear Installations.
Schwer, L., 2010. *An introduction to the Winfrith Concrete Model.* [En ligne].
Trentacoste, M., 2007. *Users Manual for LS-DYNA Concrete: Material Model 159,* s.l.: U.S. Department of transportation.
Wu, Y., Crawford, J. E. & Magallanes, J. M., 2012. *Performance of LS-DYNA Concrete Constitutive Models.* Dearborn, s.n.